NANO LETTERS

pubs.acs.org/NanoLett Letter

Activation and Assembly of Plasmonic-Magnetic Nanosurfactants for Encapsulation and Triggered Release

Fei Liu, Yifan Li, Yanhua Huang, Ayuna Tsyrenova, Kyle Miller, Lin Zhou, Hantang Qin, and Shan Jiang*

Cite This: https://dx.doi.org/10.1021/acs.nanolett.0c03641 Read Online

ACCESS | Metrics & More | Article Recommendations | Supporting Information

ABSTRACT: Multifunctional surfactants hold great potentials in catalysis, separation, and biomedicine. Highly active plasmonic-magnetic nanosurfactants are developed through a novel acid activation treatment of Au−Fe_3O_4 dumbbell nanocrystals. The activation step significantly boosts nanosurfactant surface energy and enables the strong adsorption at interfaces, which reduces the interfacial energy one order of magnitude. Mediated through the adsorption at the emulsion interfaces, the nanosurfactants are further constructed into free-standing hierarchical structures, including capsules, inverse capsules, and two-dimensional sheets. The nanosurfactant orientation and assembly structures follow the same packing parameter principles of surfactant molecules. Furthermore, nanosurfactants demonstrate the capability to disperse and encapsulate homogeneous nanoparticles and small molecules without adding any molecular surfactants. The assembled structures are responsive to external magnetic field, and triggered release is achieved using an infrared laser by taking advantage of the enhanced surface plasmon resonance of nanosurfactant assemblies. Solvent and pH changes are also utilized to achieve the cargo release.

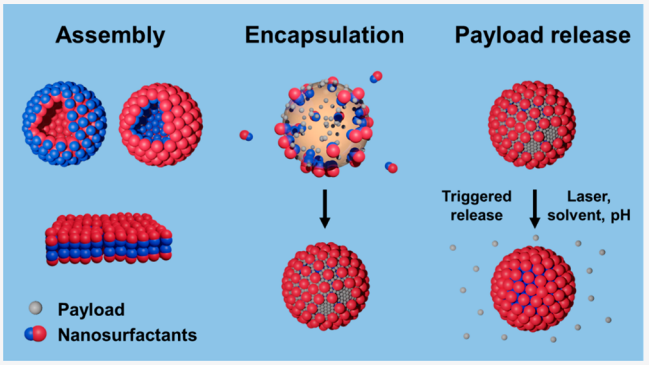

KEYWORDS: *surfactants, surface adsorption, self-assembly, encapsulation, triggered release*

Surfactant molecules are widely used in dispersing particles, stabilizing phases, and encapsulating reagents for transportation and delivery due to their capabilities of adsorption and reduction of interfacial tension.[1] For example, surfactants are often employed to disperse immiscible phases and encapsulate nanoparticles as functional components for diagnostics and drug delivery.[2,3] Stabilization of nanoparticles is critical to their broad applications, since the formation of random aggregates due to high surface area and strong interparticle attractions is detrimental to material performance.[4−6] However, weak adsorption of small surfactant molecules may not provide enough stabilization for nanoparticles, especially when nanoparticle concentration is high.[7,8] In addition, their diffusive nature also causes concerns of contamination, toxicity, and durability in applications such as coatings, personal care, and drug formulations.[9−11] Furthermore, advanced surfactants combining multiple functionalities, e.g., magnetic and optical properties, are highly desirable for building smart systems that are responsive to the environment.[12] However, it is currently challenging to integrate these functionalities into surfactant molecules.

A concept of nanosurfactants, combining the enhanced adsorption power and multifunctionality of nanoparticles, may help address these challenges. Inspired by the amphiphilic nature of surfactant molecules, we define nanosurfactants as amphiphilic nanoparticles with a Janus geometry that can adsorb strongly at the interfaces. Like the surfactant structure, one side of the nanosurfactant is hydrophilic while the other side is hydrophobic. This Janus feature differentiates nanosurfactants from conventional homogeneous colloidal particles with intermediate hydrophobicity or surfactant-coated nanoparticles.[13] More importantly, the balance between hydrophobic and hydrophilic sides, termed the Janus balance, can be tuned to control the amphiphilicity of nanosurfactants.[14,15] However, it is not a trivial task to synthesize nanosurfactants with well-defined morphology and highly active surfaces.

Recently, dumbbell-like nanoparticles have emerged as a potential candidate for fabricating multifunctional nanosurfactants.[16,17] The two lobes on the dumbbell nanoparticles can be rendered one hydrophilic and the other one hydrophobic to achieve the amphiphilicity.[18−20] The dumbbell

Received: September 9, 2020
Revised: November 6, 2020

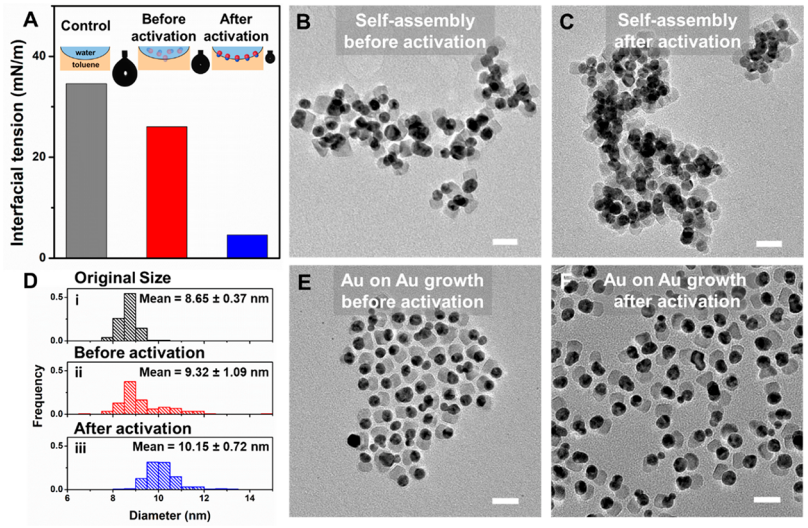

Figure 1. (A) Interfacial tension of a water droplet in toluene with Au−Fe_3O_4 nanoparticles before and after activation. (B,C) TEM images of self-assembly of Au−Fe_3O_4 nanoparticles in aqueous suspension (B) before and (C) after activation. (D) Average Au size of (i) Au−Fe_3O_4 nano-dumbbells and (ii, iii) Au−Au−Fe_3O_4 heterostructures synthesized from Au−Fe_3O_4 nano-dumbbells before and after activation. TEM images of Au−Au−Fe_3O_4 heterostructures obtained by growing Au domains on Au−Fe_3O_4 nano-dumbbells (E) before and (F) after activation. Scale bar, 20 nm.

shape is typically obtained via the seeded-growth method, and the amphiphilicity is achieved through the selective ligand exchanges on the two lobes. However, the dumbbell formation and coverage of the second lobe on the first lobe is sensitive to the synthesis conditions.[21−25] For example, materials from the second lobe growth may deposit on the exposed area of the seed lobe and form a thin, hard-to-detect layer.[26] Even a small quantity of deposition could partially or completely block the surface of the seed nanoparticles from further modification.[26] As a result, ligand exchange could fail to produce amphiphilic dumbbell-like nanoparticles, even though they present an asymmetric morphology.[27,28] In addition, adsorption at the oil−water interface alone cannot validate the asymmetric modification of nano-dumbbells, since homogeneous nanoparticles may also adsorb strongly at the interface with amphiphilic ligands. One way to verify the nanosurfactants is to study their orientations in assembly structures or at the interface.

In this study, we developed a critical activation step to improve the amphiphilicity of Au−Fe_3O_4 dumbbell-like nanosurfactants through an acid cleansing treatment. The assembly structures and interfacial adsorption of nanosurfactants were significantly improved after activation. Both oil-in-water and water-in-oil emulsion droplets could be stabilized by nanosurfactants without any additional molecular surfactants. In addition, electron microscopy images clearly indicated that the orientation of the nanosurfactants at the droplet interface was consistently reversed when the emulsion phase was inverted. Assembly structures of nanosurfactants, including capsules, inverse capsules, and sheets, were obtained by an emulsion-mediated process and demonstrated unique plasmonic resonance responses. Furthermore, due to their superior stabilizing power the nanosurfactants were applied to encapsulate diverse payloads, including homogeneous nanoparticles and small molecules with different hydrophobicity. Taking advantage of the surface-enhanced plasmon resonance (SPR) effect, the payloads in the encapsulated structures could be trigger-released by near infrared (NIR) laser irradiation. These unique features of nanosurfactants may be beneficial to many applications, including targeted drug delivery and controlled release.

Au−Fe_3O_4 nanoparticles were synthesized, activated by an acid cleansing treatment and further selectively functionalized to prepare active nanosurfactants (more details can be found in the Supporting Information). To compare the interfacial activity of Au−Fe_3O_4 nanoparticles before and after activation, interfacial tension between water and toluene in the presence of nanoparticles was studied using a pendant drop tensiometry (Figure 1A). Without acid treatment, Au−Fe_3O_4 nanoparticles only reduced the interfacial tension between water and toluene by ∼25% (from 34.6 to 26.1 mN/m). In contrast, the activated nanosurfactants significantly reduced the interfacial tension one order of magnitude (to 4.6 mN/m), indicating that these nanoparticles are much more interfacially active. Compared to other nanoparticle-based surfactants[29] and conventional surfactants,[30] our Au−Fe_3O_4 nanosurfactants exhibited comparable ability to reduce the interfacial tension, suggesting their potential for emulsion stabilization and drug delivery applications. Self-assembly of Au−Fe_3O_4 nanoparticles in aqueous solutions before and after activation was used to further compare their surface activities. As seen in Figure 1B, Au−Fe_3O_4 nanoparticles before activation only assembled into small clusters (e.g., dimers, trimers, and tetramers) with their Au lobes facing each other. These structures are similar to those observed in our previous work.[19] After activation, Au−Fe_3O_4 nanoparticles assembled into much bigger wormlike clusters, still with the hydrophobic Au lobes staying together (Figure 1C). Similar structures have only been previously observed in highly amphiphilic micron-size Janus particles.[31] These assembly structures are analogous to the micelles formed by surfactant molecules with different packing parameters,[32,33] which are only possible when hydrophobic sides strongly attract each other. Therefore, activation is critical in producing nanosurfactants with enhanced amphiphilicity and attractions among hydrophobic (Au) lobes. As a result, the plasmonic coupling of nanosurfactants was strongly improved (Figure S2). A clear red shift in SPR band was found for assembled nanosurfactants after activation. Since homogenous

https://dx.doi.org/10.1021/acs.nanolett.0c03641
Nano Lett. XXXX, XXX, XXX−XXX

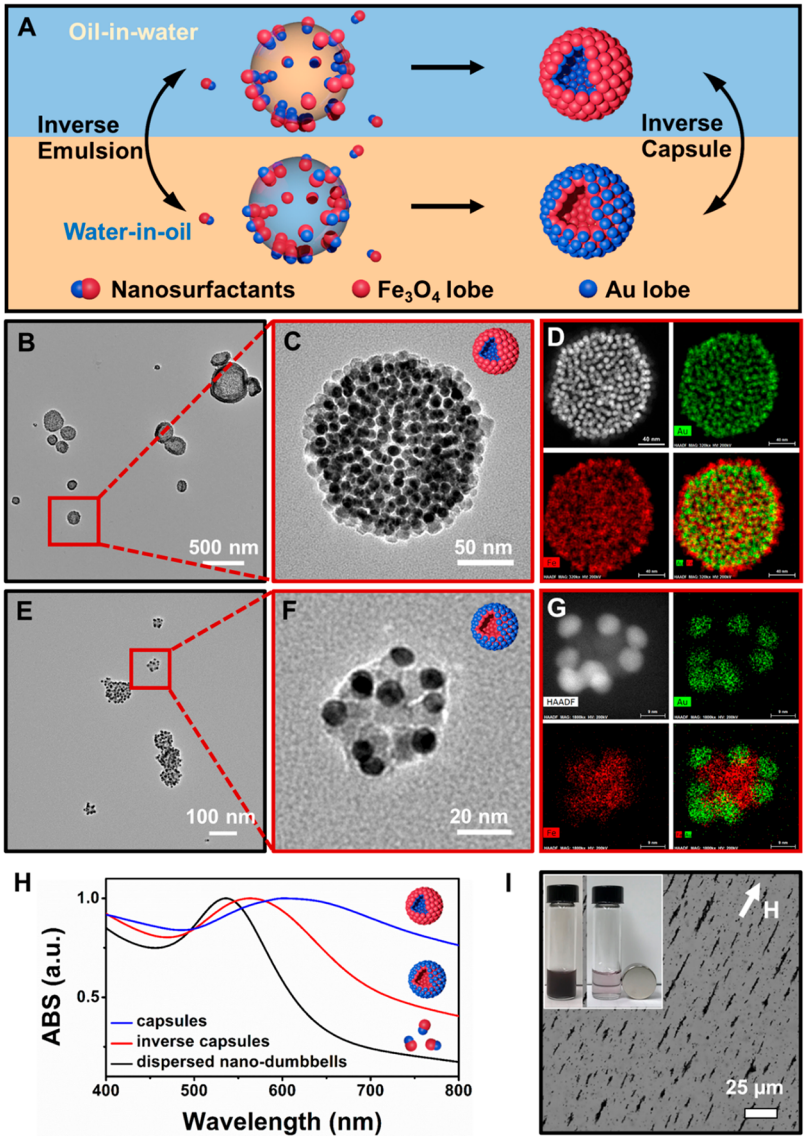

Figure 2. (A) Schematic illustration of reversible assembly of nanosurfactants mediated by oil/water interface. (B,C) TEM images of Au−Fe_3O_4 capsules at different magnifications. (D) HAADF-STEM image and corresponding EDS elemental mapping of a typical Au−Fe_3O_4 capsule. (E,F) TEM images of Au−Fe_3O_4 inverse capsules. (G) HAADF-STEM image and corresponding EDS elemental mapping of a typical Au−Fe_3O_4 inverse capsule. (H) UV−vis spectra of dispersed Au−Fe_3O_4 nano-dumbbells, Au−Fe_3O_4 capsules, and inverse capsules. (I) Optical microscope image of capsules under an external magnetic field. The inset is the optical image of Au−Fe_3O_4 capsules in the solution in the absence and presence of an external magnet for 5 min.

nanoparticles after acid treatment exhibit very similar SPR (Figure S3), the red shift of SPR band in assembled nanosurfactants is mainly due to stronger plasmonic coupling of the Au lobes in the structures.

In addition, activation boosts the reactivity of the Au lobe. This is beneficial for building more complex hybrid nanoarchitectures, such as the M−Au−Fe_3O_4 (M = Au, Pt, Ag, etc.) heterostructures using Au−Fe_3O_4 nano-dumbbells as seed particles, bringing more opportunities in catalysis, sensing, and biomedicine.[28] For example, the growth of additional Au domain on Au−Fe_3O_4 further offers an effective way to enlarge the Au side and tune SPR of Au−Fe_3O_4 nano-dumbbells. As shown in Figure 1E, small Au domains were observed on the Au lobe of Au−Fe_3O_4 nanoparticles without any acid treatment. However, the evolved Au-on-Au lobe morphology only slightly enlarges the average size of Au lobe from 8.65 to 9.32 nm (Figure 1D), implying that the reactivity of Au−Fe_3O_4 nanoparticles before acid treatment is limited. In contrast, after acid treatment, the additional Au growth led to the Au lobe with a size of 10.15 nm (Figure 1D,F), indicating an improved surface reactivity. This can be attributed to more accessible Au nucleation sites after removing the iron species on the Au surface of nano-dumbbells via acid treatment. Furthermore, a more red-shifted and broader SPR band of Au−Au−Fe_3O_4 heterostructures from acid activated Au−Fe_3O_4 nano-dumbbells was observed compared to those from Au−Fe_3O_4 without activation (Figure S4).

Analogous to conventional small molecular surfactants, nanosurfactants are capable of stabilizing both oil-in-water and water-in-oil emulsions (Figure S5). Because the nanosurfactants are strongly anchored at the water/oil interface, the interface thus can act as a template for the nanosurfactants to orient and assemble. By collapsing the emulsion via sonication and centrifugation, nanosurfactants assembled into free-

https://dx.doi.org/10.1021/acs.nanolett.0c03641
Nano Lett. XXXX, XXX, XXX−XXX

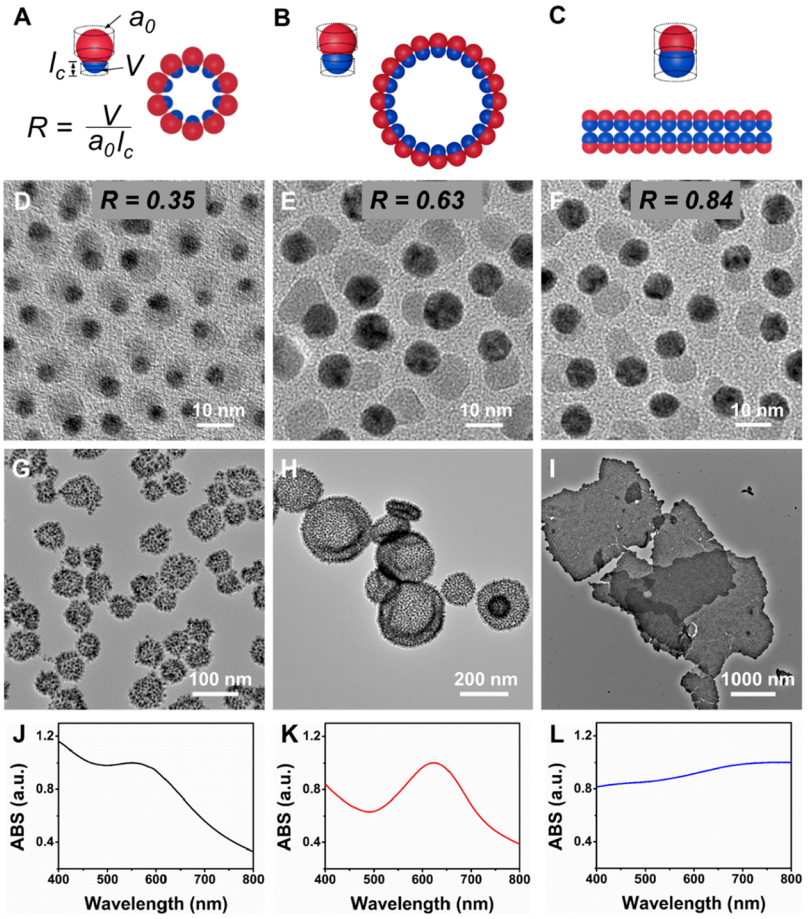

Figure 3. (A–C) Cross-sectional views of various structures from self-assembly of nanosurfactants with different Janus balance and packing parameters. TEM images of Au–Fe_3O_4 dumbbell-like nanoparticles with packing parameter of (D) 0.35, (E) 0.63, and (F) 0.84 and (G–I) their corresponding self-assemblies. (J–L) UV–vis spectra of nanosurfactants assemblies showing in (D–F).

standing capsule-like clusters (Figure 2A). For clusters formed from oil-in-water emulsions, nanosurfactants orient with their hydrophilic lobes facing outward while hydrophobic lobes face inward toward each other (Figure 2B,C). The orientation was further confirmed by high-angle annular dark-field scanning transmission electron microscopy (HAADF-STEM) images and corresponding energy dispersive spectroscopy (EDS) elemental mapping (Figure 2D). The orientation matches the hydrophobicity preference at the emulsion interface, which means nanosurfactant orientation is preserved even after liquid phases evaporate. Most likely, the fixation in configuration and orientation is due to the strong van der Waals (VDW) attractions between nanosurfactant particles (more discussions can be found in Supporting Information). In contrast to the oil-in-water emulsions, the inverse water-in-oil emulsions led to clusters with reversed lobe orientations, as confirmed by TEM, HAADF-STEM imaging and EDS elemental mapping analysis (Figure 2E–G). More interestingly, the structures are even reversible when the emulsions are re-established and switched. Using the same batch of nanosurfactants, the assemblies were reversed several times without forming any noticeable random aggregations. These observations on nanosurfactant orientation provide further evidence for the successful asymmetric rendition of nano-dumbbells.

Owing to their Au and Fe_3O_4 components, nanosurfactants possessed unique dual plasmonic-magnetic properties that are rarely found in conventional molecular surfactants. Self-assembly of nanosurfactants into capsules further engaged stronger plasmonic and magnetic coupling between Au and Fe_3O_4 domains. Both Au–Fe_3O_4 capsules and inverse capsules showed clear red shift in the SPR band compared to dispersed Au–Fe_3O_4 nano-dumbbells, indicating improved plasmonic coupling (Figure 2H). Interestingly, capsules exhibited stronger absorption in the NIR region and greater red shift than that of inverse capsules, which can be attributed to Au face-to-face configuration and shorter Au–Au distance in the capsules. In comparison with dispersed nano-dumbbells, capsules also showed stronger magnetic response, as confirmed by the faster separation from the solution in the presence of an external magnet (Figure 2I and Figure S6). The magnetic field could also induce the attachment and alignment of capsules (Figure 2I). The unique plasmonic-magnetic property and biocompatible ingredients of nanosurfactants offer their great potential in drug delivery and controlled release.[20,34]

The size of clusters can be controlled by Janus balance of nanosurfactants. Here, Janus balance is defined as the ratio of radius between Au and Fe_3O_4 lobes, which can be viewed as the counterpart of the HLB (hydrophilic–lipophilic balance) for molecular surfactants.[14] It is known that the HLB is directly related to the packing parameter, which determines the morphology of micelles formed by molecular surfactants.[32] Figure 3 shows the nanosurfactants with different Janus balances and their corresponding free-standing assembly structures formed through the oil-in-water emulsions. The

https://dx.doi.org/10.1021/acs.nanolett.0c03641
Nano Lett. XXXX, XXX, XXX–XXX

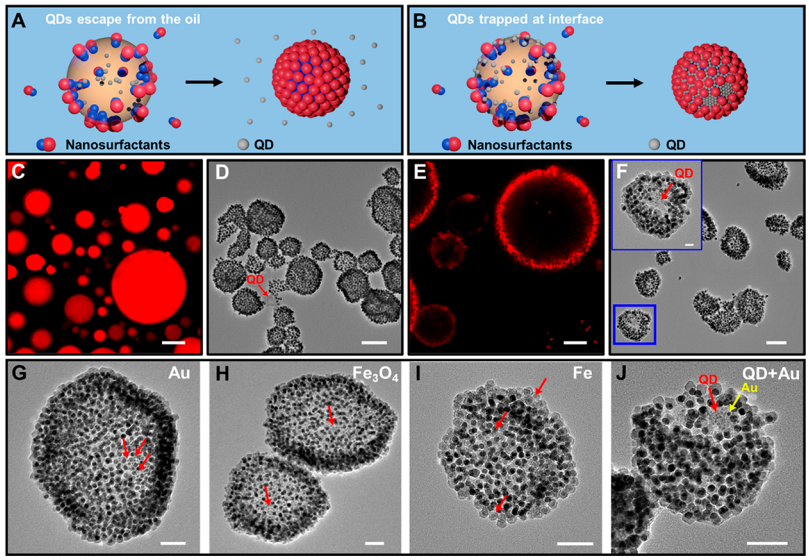

Figure 4. Schematic illustrations of (A) unsuccessful and (B) successful encapsulation of QDs by nanosurfactants. (C) Confocal laser scanning microscopy image of nanosurfactants stabilized droplets containing CdSe QDs. Scale bar, 10 μm. (D) TEM image of leached CdSe QDs. Scale bar, 100 nm. (E) Confocal laser scanning microscopy image of nanosurfactants stabilized droplets with CdSe QDs at the interface. Scale bar, 10 μm. (F) TEM image of successful encapsulation with CdSe QDs trapped in nanosurfactant assemblies. Scale bar, 100 nm. The inset is a zoomed-in image of the blue square. Scale bar, 20 nm. (G–J) TEM images of encapsulation of (G) Au, (H) Fe_3O_4, (I) Fe, and (J) CdSe QDs and Au by nanosurfactants. Arrows indicate the positions of encapsulated nanoparticles. Scale bars, 50 nm.

packing parameter for nanosurfactant is derived similarly to small surfactant molecules, defined as $R = V/a_0l_c$, where V is the volume of the Au lobe, a_0 is the cross-sectional area of the Fe_3O_4 lobe, and l_c is height of the Au lobe (Figure 3A–C). The calculated values based on measurement in TEM images are shown in Figure 3D–F. nanosurfactants with the smallest Janus balance and packing parameter assembled into capsule-like clusters of ~70 nm (Figure 3G). As the Janus balance was gradually tuned from 0.59 to 0.92, the packing parameter R increased from 0.35 to 0.84. Correspondingly, the observed curvatures of the assembly structures decreased, and the average size of the assembly increased to ~200 nm (Figure 3H and Figure S7). The dynamic light scattering measurement also indicates an increased hydrodynamic size of assembly strucutures when Janus balance is increased (Figure S8). It is worth emphasizing that in both cases highly concerted orientations are noticeable with the Au lobes orienting toward each other whereas the Fe_3O_4 lobes face outward. UV–vis spectroscopy revealed that larger capsules exhibited stronger SPR effect because of their larger Au size and more Au lobes staying close (Figure 3J,K). When Janus balance was adjusted to 0.92, two-dimensional sheetlike structures were obtained (Figure 3I and Figures S9 and S10). The thickness of the sheets was measured by atomic force microscopy (Figure S11) to be ~40 nm, twice the size of nanosurfactants, implying the formation of a bilayer of Au–Fe_3O_4 nanosurfactants. The sheets showed broad SPR band into the NIR region, probably due to their bilayer structure and micron size (Figure 3L). The observed trend in structural evolution of nanosurfactant self-assembly mirrors that of small molecular surfactants.[32] Further discussions on emulsion stabilization by nanosurfactants can be found in Supporting Information.

Encapsulation of drugs, functional nanoparticles, and cells by molecular surfactants and polymers have been widely applied in various biomedical applications.[35,36] Environmentally responsive systems (e.g., light, temperature, ultrasound, and magnetic field) are highly desirable for on-demand and precise therapy.[37] Here, the superior stabilizing power and unique self-assembly of nanosurfactants offer the possibility of encapsulating homogeneous nanoparticles and small molecules without adding any molecular surfactants. CdSe quantum dots (QDs, Figure S12A) were employed as model hydrophobic nanoparticles and utilized for encapsulation (Figure 4A,B). QDs were initially encapsulated in the chloroform droplets stabilized by Au–Fe_3O_4 nanosurfactants, as indicated by the confocal microscope image (Figure 4C). Au–Fe_3O_4 nanosurfactants possessed strong interfacial activity, ensuring effective encapsulation of nanoparticles in droplets. However, when the droplets were collapsed during the drying process, QDs were found to leach out from the droplets and separate from nanosurfactant assemblies (Figure 4D). This is likely due to the strong tendency for QDs to stay with the chloroform phase. In order to prevent the QDs escape and preserve strong interaction between QDs and nanosurfactants, pH of the water phase was adjusted from neutral to 10. An assisting solvent (e.g., *N*,*N*-dimethylformamide) miscible with both water and chloroform was also introduced. As a result, QDs migrated to the chloroform/water interface, which is confirmed by confocal microscopy (Figure 4E). This could be due to the partially charged surface induced by strong OH^- ion adsorption.[38,39] The assisting solvent was also found important to facilite the OH^- ion adsorption. In this way, both nanosurfactants and QDs were anchored to the chloroform/water interface, and no leaching of QDs was observed (Figure 4F and Figure S13). During the drying process, QDs may stay closely with the nanosurfactants, and VDW forces and hydrophobic interactions prevent QDs from leaving the structures even as chloroform evaporates away.

On the basis of similar procedures, other types of nanoparticles, including Au, Fe_3O_4, and Fe[40] nanoparticles with various sizes, were successfully encapsulated by nanosurfactants, as shown in the TEM images (Figure 4G–I and Figure S12). A dual encapsulation (Au and QDs) was also realized (Figure 4J). In addition, hydrophilic nanoparticles

https://dx.doi.org/10.1021/acs.nanolett.0c03641
Nano Lett. XXXX, XXX, XXX–XXX

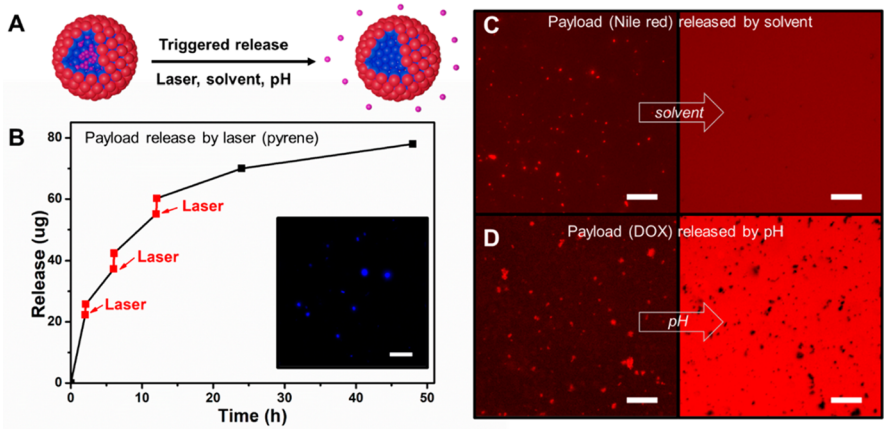

Figure 5. (A) Schematic illustration of payload release triggered by laser, solvent, and pH. (B) Release profile of pyrene from nanosurfactants encapsulation. The inset is the fluorescent image showing pyrene encapsulated by nanosurfactants. Scale bar, 20 μm. (C,D) Fluorescent images showing Nile red and DOX encapsulation and release triggered by solvent and pH, respectively. Scale bar, 20 μm.

(e.g., CdSe QDs and Fe nanoparticles) can also be encapsulated by nanosurfactants when water-in-oil emulsion is utilized (Figure S14). It is important to note that the encapsulation of all nanoparticles with nanosurfactants is achieved without any additional small molecular surfactants. The encapsulation is stable against aggregation in aqueous suspension for extended periods.

Activated Au−Fe_3O_4 nanosurfactants are capable of encapsulating various small molecules as well. A few model molecules, including Nile red, pyrene, and Doxorubicin (DOX), were successfully encapsulated using nanosurfactants (Figure 5). The encapsulation was based on the oil-in-water emulsion in which hydrophobic molecules were enriched in the oil phase. When nanosurfactants assembled into confined clusters after the oil phase was driven out of the emulsions, the molecules were trapped in the nanosurfactant assemblies. It is noted that the encapsulation of small molecules does not require a pH adjustment, unlike the encapsulation of nanoparticles.

Several mechanisms including laser irradiation, solvent change, and pH adjustment were tested to trigger the release of payloads from Au−Fe_3O_4 nanosurfactants encapsulation for potential controlled release applications (Figure 5A). First, pyrene was used as a fluorescent model molecule to quantify its release triggered by an NIR laser. As shown in Figure 5B, pyrene was constantly released over time by diffusion. Under a brief exposure to an 808 nm laser, a burst of release (highlighted in red) was observed. This can be attributed to the increased temperature caused by the photothermal effect of the nanosurfactant assemblies due to their unique SPR properties.[41] Higher temperature promotes the diffusion and solubility of pyrene in the aqueous solutions. As NIR light features high penetrability into tissues, our NIR responsive platform shows potential for remotely controlled drug delivery. Second, DMF was employed as the solvent to trigger the Nile red release. It can be seen in Figure 5C that fluorescence was initially enriched in the nanosurfactants clusters. By adding 5% DMF into the water, the solubility of Nile red in solution is increased, resulting in a gradual fluorescence increase in the background. The clusters also showed a much weaker fluorescence signal after DMF was added. Third, pH adjustment was utilized to trigger the payload release. Hydrophobic DOX was initially prepared by deprotonating DOX·HCl with the excess amount of triethylamine. DOX was then encapsulated by nanosurfactants through an oil-in-water emulsion, which was shown by the clusters enriched by fluorescent signals from the DOX (Figure 5D). When the pH was changed from neutral to acidic (~4), DOX was shifted from deprotonation to protonation state, which significantly improved its water solubility. As a result, DOX was rapidly released, indicated by the drastic fluorescence intensity increase in the background. In contrast, nanosurfactant clusters did not show any fluorescence overlap with DOX, which further implies the release of DOX from encapsulation. A similar concept of triggered release was achieved in the inverse condition when hydrophilic nanoparticles or molecules were encapsulated by nanosurfactants using a water-in-oil emulsion, and the clusters were eventually suspended in the oil phase after water evaporation (Figure S15). In addition, the intrinsic magnetic properties provided by the Fe_3O_4 lobe may offer the possibility to remotely release the payloads by an alternating magnetic field.[42]

In summary, a highly active nanosurfactant platform is established based on the fabrication of Au−Fe_3O_4 dumbbell nanocrystals and the subsequent acid cleansing treatment. These nanosurfactants demonstrate similar assembly and adsorption behaviors to small molecular surfactants. The orientations of nanosurfactants in the capsule and inverse capsule structures are consistent with the corresponding orientations of molecular surfactants. The assembly structures of nanosurfactants are also influenced by their packing parameter analogous to small surfactant molecules. Strong VDW forces help secure the structures formed by nanosurfactants in emulsions into free-standing structures when liquid phases evaporate. At the same time, the assembly structures remain dynamic and reversible when new phases and emulsions are introduced. On the other hand, nanosurfactants differ in the procedure and mechanism of dispersing and encapsulating homogeneous nanoparticles. A co-adsorption scheme is found to encapsulate homogeneous nanoparticles more successfully without any leaching. Nanosurfactants were also applied to encapsulate small molecules (Nile red, DOX, and pyrene). The encapsulated small molecules were released by different triggering mechanisms, taking advantage of the unique physical and optical properties of nanosurfactants made from Au−Fe_3O_4 nanoparticles. The newly developed nanosurfactant platform greatly expands the functionality of conventional surfactant molecules. The insight

https://dx.doi.org/10.1021/acs.nanolett.0c03641
Nano Lett. XXXX, XXX, XXX−XXX

provided by nanosurfactant interactions and assembly structures in this study paves the way for their future applications.

■ ASSOCIATED CONTENT

Supporting Information

The Supporting Information is available free of charge at https://pubs.acs.org/doi/10.1021/acs.nanolett.0c03641.

Materials and methods, discussion on preparation of nanosurfactants, nanosurfactant self-assembly and emulsion stabilization by nanosurfactants, Figure S1−S15, and additional references (PDF)

■ AUTHOR INFORMATION

Corresponding Author

Shan Jiang − *Department of Materials Science and Engineering and Department of Industrial and Manufacturing Systems Engineering, Iowa State University, Ames, Iowa 50011, United States; Division of Materials Science and Engineering, Ames Laboratory, Ames, Iowa 50011, United States;* orcid.org/0000-0001-8119-9012; Email: sjiang1@iastate.edu

Authors

Fei Liu − *Department of Materials Science and Engineering, Iowa State University, Ames, Iowa 50011, United States*

Yifan Li − *Department of Materials Science and Engineering, Iowa State University, Ames, Iowa 50011, United States*

Yanhua Huang − *Department of Materials Science and Engineering, Iowa State University, Ames, Iowa 50011, United States*

Ayuna Tsyrenova − *Department of Materials Science and Engineering, Iowa State University, Ames, Iowa 50011, United States*

Kyle Miller − *Department of Materials Science and Engineering, Iowa State University, Ames, Iowa 50011, United States*

Lin Zhou − *Department of Materials Science and Engineering, Iowa State University, Ames, Iowa 50011, United States; Division of Materials Science and Engineering, Ames Laboratory, Ames, Iowa 50011, United States;* orcid.org/0000-0003-2286-6510

Hantang Qin − *Department of Industrial and Manufacturing Systems Engineering, Iowa State University, Ames, Iowa 50011, United States;* orcid.org/0000-0003-4180-7911

Complete contact information is available at: https://pubs.acs.org/10.1021/acs.nanolett.0c03641

Notes

The authors declare no competing financial interest.

■ ACKNOWLEDGMENTS

This work is supported by Iowa State University Start-up Fund, Presidential Interdisciplinary Research Seed (PIRS) Grant, and 3M Non-tenured Faculty Award. Acknowledgment is made to the donors of the American Chemical Society Petroleum Research Fund for partial support of this research (Grant 60264-DNI7). This project/material is based upon work supported by the Iowa Space Grant Consortium under NASA Award No. 80NSSC20M0107. Part of the TEM work was performed using instruments in the Sensitive Instrument Facility in Ames Laboratory.

■ REFERENCES

(1) Myers, D. *Surfactant science and technology*, 3rd ed.; John Wiley & Sons: Hoboken, New Jersey, 2006.

(2) Kumar, G. P.; Rajeshwarrao, P. Nonionic surfactant vesicular systems for effective drug delivery—an overview. *Acta Pharm. Sin. B* **2011**, *1* (4), 208−219.

(3) Baret, J. C. Surfactants in droplet-based microfluidics. *Lab Chip* **2012**, *12* (3), 422−33.

(4) Boles, M. A.; Engel, M.; Talapin, D. V. Self-Assembly of Colloidal Nanocrystals: From Intricate Structures to Functional Materials. *Chem. Rev.* **2016**, *116* (18), 11220−11289.

(5) Min, Y. J.; Akbulut, M.; Kristiansen, K.; Golan, Y.; Israelachvili, J. The role of interparticle and external forces in nanoparticle assembly. *Nat. Mater.* **2008**, *7* (7), 527−538.

(6) Boles, M. A.; Ling, D.; Hyeon, T.; Talapin, D. V. The surface science of nanocrystals. *Nat. Mater.* **2016**, *15* (2), 141−53.

(7) Studart, A. R.; Amstad, E.; Gauckler, L. J. Colloidal Stabilization of Nanoparticles in Concentrated Suspensions. *Langmuir* **2007**, *23* (3), 1081−1090.

(8) He, S.; Chen, H.; Guo, Z.; Wang, B.; Tang, C.; Feng, Y. High-concentration silver colloid stabilized by a cationic gemini surfactant. *Colloids Surf., A* **2013**, *429*, 98−105.

(9) Cserháti, T.; Forgács, E.; Oros, G. Biological activity and environmental impact of anionic surfactants. *Environ. Int.* **2002**, *28* (5), 337−348.

(10) Rosso, D.; Huo, D. L.; Stenstrom, M. K. Effects of interfacial surfactant contamination on bubble gas transfer. *Chem. Eng. Sci.* **2006**, *61* (16), 5500−5514.

(11) Jiang, S.; Van Dyk, A.; Maurice, A.; Bohling, J.; Fasano, D.; Brownell, S. Design colloidal particle morphology and self-assembly for coating applications. *Chem. Soc. Rev.* **2017**, *46* (12), 3792−3807.

(12) Grzybowski, B. A.; Fitzner, K.; Paczesny, J.; Granick, S. From dynamic self-assembly to networked chemical systems. *Chem. Soc. Rev.* **2017**, *46* (18), 5647−5678.

(13) Binks, B. P. Colloidal Particles at a Range of Fluid−Fluid Interfaces. *Langmuir* **2017**, *33* (28), 6947−6963.

(14) Jiang, S.; Granick, S. Janus balance of amphiphilic colloidal particles. *J. Chem. Phys.* **2007**, *127* (16), 161102.

(15) Jiang, S.; Granick, S. Controlling the Geometry (Janus Balance) of Amphiphilic Colloidal Particles. *Langmuir* **2008**, *24* (6), 2438−2445.

(16) Wang, C.; Xu, C. J.; Zeng, H.; Sun, S. H. Recent Progress in Syntheses and Applications of Dumbbell-like Nanoparticles. *Adv. Mater.* **2009**, *21* (30), 3045−3052.

(17) Yang, T.; Wei, L.; Jing, L.; Liang, J.; Zhang, X.; Tang, M.; Monteiro, M. J.; Chen, Y.; Wang, Y.; Gu, S.; Zhao, D.; Yang, H.; Liu, J.; Lu, G. Q. M. Dumbbell-Shaped Bi-component Mesoporous Janus Solid Nanoparticles for Biphasic Interface Catalysis. *Angew. Chem., Int. Ed.* **2017**, *56* (29), 8459−8463.

(18) Li, Y.; Chen, S.; Demirci, S.; Qin, S.; Xu, Z.; Olson, E.; Liu, F.; Palm, D.; Yong, X.; Jiang, S. Morphology evolution of Janus dumbbell nanoparticles in seeded emulsion polymerization. *J. Colloid Interface Sci.* **2019**, *543*, 34−42.

(19) Liu, F.; Goyal, S.; Forrester, M.; Ma, T.; Miller, K.; Mansoorieh, Y.; Henjum, J.; Zhou, L.; Cochran, E.; Jiang, S. Self-assembly of Janus Dumbbell Nanocrystals and Their Enhanced Surface Plasmon Resonance. *Nano Lett.* **2019**, *19* (3), 1587−1594.

(20) Song, J. B.; Wu, B. H.; Zhou, Z. J.; Zhu, G. Z.; Liu, Y. J.; Yang, Z.; Lin, L. S.; Yu, G. C.; Zhang, F. W.; Zhang, G. F.; Duan, H. W.; Stucky, G. D.; Chen, X. Y. Double-Layered Plasmonic-Magnetic Vesicles by Self-Assembly of Janus Amphiphilic Gold-Iron(II,III) Oxide Nanoparticles. *Angew. Chem., Int. Ed.* **2017**, *56* (28), 8110−8114.

(21) Jiang, G.; Huang, Y.; Zhang, S.; Zhu, H.; Wu, Z.; Sun, S. Controlled synthesis of Au-Fe heterodimer nanoparticles and their conversion into Au-Fe3O4 heterostructured nanoparticles. *Nanoscale* **2016**, *8* (41), 17947−17952.

(22) Liu, S.; Guo, S. J.; Sun, S.; You, X. Z. Dumbbell-like Au-Fe3O4 nanoparticles: a new nanostructure for supercapacitors. *Nanoscale* **2015**, *7* (11), 4890−4893.
(23) Yu, H.; Chen, M.; Rice, P. M.; Wang, S. X.; White, R. L.; Sun, S. H. Dumbbell-like bifunctional Au-Fe3O4 nanoparticles. *Nano Lett.* **2005**, *5* (2), 379−382.
(24) Zhang, H.; Yang, Z.; Ju, Y.; Chu, X.; Ding, Y.; Huang, X.; Zhu, K.; Tang, T.; Su, X.; Hou, Y. Galvanic Displacement Synthesis of Monodisperse Janus- and Satellite-Like Plasmonic−Magnetic Ag−Fe@Fe3O4 Heterostructures with Reduced Cytotoxicity. *Adv. Sci.* **2018**, *5* (8), 1800271.
(25) Ju, Y.; Zhang, H.; Yu, J.; Tong, S.; Tian, N.; Wang, Z.; Wang, X.; Su, X.; Chu, X.; Lin, J.; Ding, Y.; Li, G.; Sheng, F.; Hou, Y. Monodisperse Au−Fe2C Janus Nanoparticles: An Attractive Multifunctional Material for Triple-Modal Imaging-Guided Tumor Photothermal Therapy. *ACS Nano* **2017**, *11* (9), 9239−9248.
(26) Hodges, J. M.; Biacchi, A. J.; Schaak, R. E. Ternary Hybrid Nanoparticle Isomers: Directing the Nucleation of Ag on Pt−Fe3O4 Using a Solid-State Protecting Group. *ACS Nano* **2014**, *8* (1), 1047−1055.
(27) Fantechi, E.; Roca, A. G.; Sepúlveda, B.; Torruella, P.; Estradé, S.; Peiró, F.; Coy, E.; Jurga, S.; Bastús, N. G.; Nogués, J.; Puntes, V. Seeded Growth Synthesis of Au−Fe3O4 Heterostructured Nanocrystals: Rational Design and Mechanistic Insights. *Chem. Mater.* **2017**, *29* (9), 4022−4035.
(28) Hodges, J. M.; Morse, J. R.; Fenton, J. L.; Ackerman, J. D.; Alameda, L. T.; Schaak, R. E. Insights into the Seeded-Growth Synthesis of Colloidal Hybrid Nanoparticles. *Chem. Mater.* **2017**, *29* (1), 106−119.
(29) Liu, X.; Kent, N.; Ceballos, A.; Streubel, R.; Jiang, Y.; Chai, Y.; Kim, P. Y.; Forth, J.; Hellman, F.; Shi, S.; Wang, D.; Helms, B. A.; Ashby, P. D.; Fischer, P.; Russell, T. P. Reconfigurable ferromagnetic liquid droplets. *Science* **2019**, *365* (6450), 264.
(30) Bąk, A.; Podgórska, W. Interfacial and surface tensions of toluene/water and air/water systems with nonionic surfactants Tween 20 and Tween 80. *Colloids Surf., A* **2016**, *504*, 414−425.
(31) Chen, Q.; Whitmer, J. K.; Jiang, S.; Bae, S. C.; Luijten, E.; Granick, S. Supracolloidal Reaction Kinetics of Janus Spheres. *Science* **2011**, *331* (6014), 199−202.
(32) Rodríguez-Abreu, C. On the Relationships between the Hydrophilic−Lipophilic Balance and the Nanoarchitecture of Nonionic Surfactant Systems. *J. Surfactants Deterg.* **2019**, *22* (5), 1001−1010.
(33) Won, Y.-Y.; Brannan, A. K.; Davis, H. T.; Bates, F. S. Cryogenic Transmission Electron Microscopy (Cryo-TEM) of Micelles and Vesicles Formed in Water by Poly(ethylene oxide)-Based Block Copolymers. *J. Phys. Chem. B* **2002**, *106* (13), 3354−3364.
(34) Reguera, J.; Jiménez de Aberasturi, D.; Henriksen-Lacey, M.; Langer, J.; Espinosa, A.; Szczupak, B.; Wilhelm, C.; Liz-Marzán, L. M. Janus plasmonic−magnetic gold−iron oxide nanoparticles as contrast agents for multimodal imaging. *Nanoscale* **2017**, *9* (27), 9467−9480.
(35) Ernst, A. U.; Bowers, D. T.; Wang, L.-H.; Shariati, K.; Plesser, M. D.; Brown, N. K.; Mehrabyan, T.; Ma, M. Nanotechnology in cell replacement therapies for type 1 diabetes. *Adv. Drug Delivery Rev.* **2019**, *139*, 116−138.
(36) Martínez Rivas, C. J.; Tarhini, M.; Badri, W.; Miladi, K.; Greige-Gerges, H.; Nazari, Q. A.; Galindo Rodríguez, S. A.; Román, R. Á.; Fessi, H.; Elaissari, A. Nanoprecipitation process: From encapsulation to drug delivery. *Int. J. Pharm.* **2017**, *532* (1), 66−81.
(37) Karimi, M.; Ghasemi, A.; Sahandi Zangabad, P.; Rahighi, R.; Moosavi Basri, S. M.; Mirshekari, H.; Amiri, M.; Shafaei Pishabad, Z.; Aslani, A.; Bozorgomid, M.; Ghosh, D.; Beyzavi, A.; Vaseghi, A.; Aref, A. R.; Haghani, L.; Bahrami, S.; Hamblin, M. R. Smart micro/nanoparticles in stimulus-responsive drug/gene delivery systems. *Chem. Soc. Rev.* **2016**, *45* (5), 1457−1501.
(38) Tamura, H.; Katayama, N.; Furuichi, R. Modeling of Ion-Exchange Reactions on Metal Oxides with the Frumkin Isotherm. 1. Acid−Base and Charge Characteristics of MnO2, TiO2, Fe3O4, and Al2O3 Surfaces and Adsorption Affinity of Alkali Metal Ions. *Environ. Sci. Technol.* **1996**, *30* (4), 1198−1204.
(39) Zeng, C.; Ramos-Ruiz, A.; Field, J. A.; Sierra-Alvarez, R. Cadmium telluride (CdTe) and cadmium selenide (CdSe) leaching behavior and surface chemistry in response to pH and O2. *J. Environ. Manage.* **2015**, *154*, 78−85.
(40) Peng, S.; Wang, C.; Xie, J.; Sun, S. Synthesis and Stabilization of Monodisperse Fe Nanoparticles. *J. Am. Chem. Soc.* **2006**, *128* (33), 10676−10677.
(41) You, J.; Zhang, G.; Li, C. Exceptionally High Payload of Doxorubicin in Hollow Gold Nanospheres for Near-Infrared Light-Triggered Drug Release. *ACS Nano* **2010**, *4* (2), 1033−1041.
(42) Oliveira, H.; Pérez-Andrés, E.; Thevenot, J.; Sandre, O.; Berra, E.; Lecommandoux, S. Magnetic field triggered drug release from polymersomes for cancer therapeutics. *J. Controlled Release* **2013**, *169* (3), 165−170.

https://dx.doi.org/10.1021/acs.nanolett.0c03641
Nano Lett. XXXX, XXX, XXX−XXX